

# Chapter 5

Synthesis and Characterization  
of  
Transition Metal (Co, Mn, Ni)-  
Substituted  
Phosphomolybdates

## Keggin-type cesium salt of first series transition metal-substituted phosphomolybdates: one-pot easy synthesis, structural, and spectral analysis

ANJALI PATEL\* and SOYEB PATHAN

Department of Chemistry, Faculty of Science, M. S. University of Baroda, Vadodara – 390002, Gujarat, India

(Received 8 March 2012; in final form 8 July 2012)

The Keggin-type cesium salt of transition metal-substituted phosphomolybdates,  $\text{Cs}_5[\text{PCo}(\text{H}_2\text{O})\text{Mo}_{11}\text{O}_{39}] \cdot 6\text{H}_2\text{O}$  (1) and  $\text{Cs}_5[\text{PMn}(\text{H}_2\text{O})\text{Mo}_{11}\text{O}_{39}] \cdot 6\text{H}_2\text{O}$  (2), were synthesized from commercially available  $\text{H}_3\text{PMo}_{12}\text{O}_{40}$ . The compounds were characterized by thermal, structural, and spectroscopic techniques. X-ray structural analysis reveals that, in these isostructural disordered compounds, the transition metal (Co/Mn) and Mo atoms are distributed over 12 positions. The presence of Co/Mn atoms was confirmed by powder XRD, FT-IR, DR-UV-Vis, ESR, and  $^{31}\text{P}$  NMR studies.

**Keywords:** Keggin; Polyoxometalates; Substituted phosphomolybdate; Cobalt; Manganese

Dalton  
Transactions

RSC Publishing

PAPER

### Keggin type mono Ni(II)-substituted phosphomolybdate: a sustainable, homogeneous and reusable catalyst for Suzuki–Miyaura cross-coupling†

Cite this: Dalton Trans., 2013, 42, 11600

Soyeb Pathan and Anjali Patel\*

Keggin type mono Ni(II)-substituted phosphomolybdate was synthesized and characterized by various physico-chemical techniques and used as a catalyst for Suzuki–Miyaura cross-coupling. The influence of different reaction parameters was studied, to get the maximum yield. The novelty of the present work lies in obtaining >97% yield of biphenyl in 14 h under mild reaction conditions. Although the present catalyst is homogeneous, it was regenerated and reused up to two cycles. Results demonstrated that the catalyst was effective and sustainable for cross-coupling of various halobenzenes with phenylboronic acid in aqueous medium.

Received 29th April 2013

Accepted 8th June 2013

DOI: 10.1039/c3dt51119g

www.rsc.org/dalton

The incorporation of various transition metal ions into POMs provides a powerful method for the structural modification and synthesis of novel metal incorporated materials that combine the features of both the transition metals as well as POM clusters. The resulting materials, TMSPOMs are useful single-site catalysts where the active metal M is isolated in, and strongly bound to, an inorganic metal-oxide matrix and thus is prevented from oligomerization and leaching [1,2].

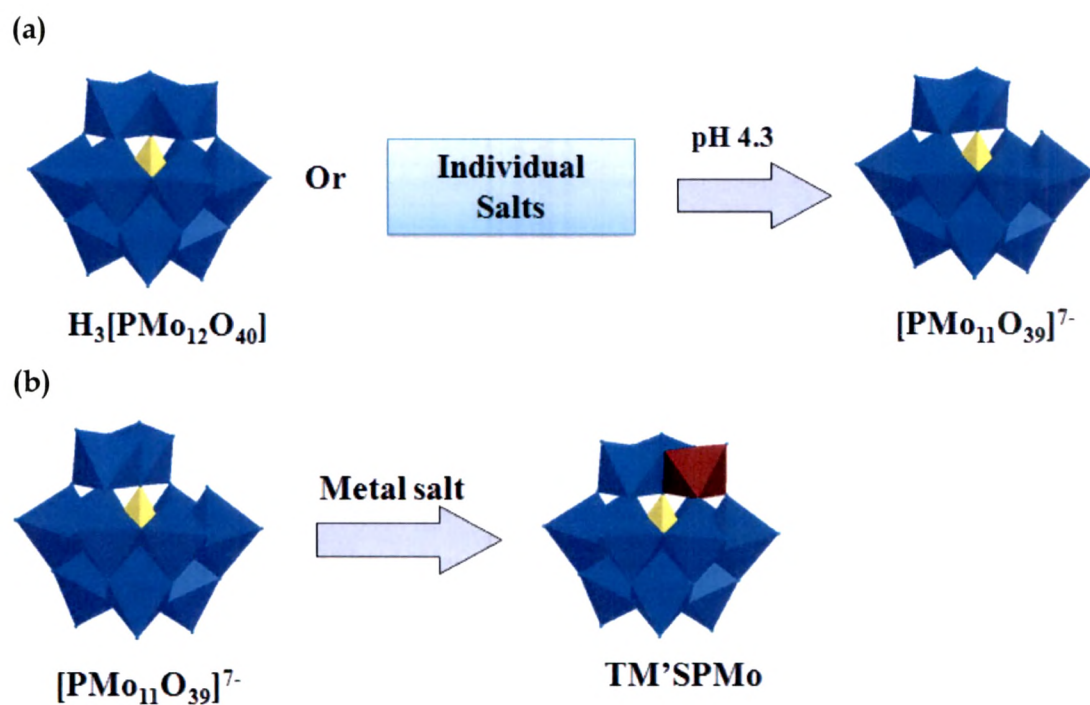
Among the various Keggin-type TMSPOMs, Cobalt-substituted POMs and Manganese substituted POMs are of interest for their variable oxidation states and redox properties [3]. A literature survey shows several reports on the synthesis and characterization of Cobalt/Manganese substituted polyoxotungstates [4-12] as well as silicotungstates [5,13-15]. At the same time, reports on analogous compounds based on phosphomolybdates are limited.

Combs-Walker and Hill reported a two-step synthesis of tetrabutyl ammonium salt of transition metal-substituted phosphomolybdates (M= Co, Mn, Cu, and Zn) [16]. They reported a biphasic extraction technique which described metalation of  $\text{TBA}_4\text{H}_3\text{-PMo}_{11}\text{O}_{39}$  with  $\text{MSO}_4$  (M= Mn, Co). Using same method, TBA salt of  $\text{PMo}_{11}\text{MO}_{40}$  (M= Co, Mn) have been synthesized by Neumann et al. [17] and karcz et al. [18].

Lin et al. reported a chain-like crystal structure of  $[(\text{CH}_3)_3\text{NH}]_{5n}[\text{PMo}_{11}\text{MO}_{39}]^n \cdot x\text{H}_2\text{O}$  (M =  $\text{Mn}^{2+}$ ,  $x = n$ ;  $\text{Co}^{2+}$ ,  $x = 2n$ ) [19]. This method involves synthesis from the individual transition metal salts (i.e.,  $\text{Na}_2\text{MoO}_4 \cdot 2\text{H}_2\text{O}$  and  $\text{Co}(\text{CH}_3\text{COO})_2$ ). They investigated electrochemical and magnetic properties of these compounds. Rabia et al. reported the synthesis of the ammonium salt of  $\text{PMo}_{11}\text{CoO}_{40}$  from individual transition metal salts (ammonium heptamolybdate, cobalt sulfate) [20].

The syntheses, crystal structures, and physical properties of a series of radical salts made with bis(ethylenedithio)tetrathiafulvalene (BEDT-TTF or ET) and  $[\text{PMn}(\text{H}_2\text{O})\text{Mo}_{11}\text{O}_{39}]^{5-}$  have been reported by Coronado et al. [21]. Hu and Burns synthesized and characterized a series of  $\text{Na}_2[(\text{C}_4\text{H}_9)_4\text{N}]_4[\text{PZ}(\text{II})(\text{Br})\text{Mo}_{11}\text{O}_{39}]$ , where  $Z = \text{Mn}(\text{II}), \text{Co}(\text{II}), \text{Ni}(\text{II}), \text{Cu}(\text{II})$  and  $\text{Zn}(\text{II})$  [22]. Recently, Cavaleiro et al. reported synthesis of  $\text{TBA}_4\text{H}[\text{PMo}_{11}\text{Mn}(\text{H}_2\text{O})\text{O}_{39}]\cdot 2\text{H}_2\text{O}$  from individual salt i.e.  $\text{Na}_2\text{MoO}_4\cdot 2\text{H}_2\text{O}$  and  $\text{Na}_2\text{HPO}_4$  and  $\text{MnSO}_4\cdot \text{H}_2\text{O}$  at  $90\text{ }^\circ\text{C}$  [23].

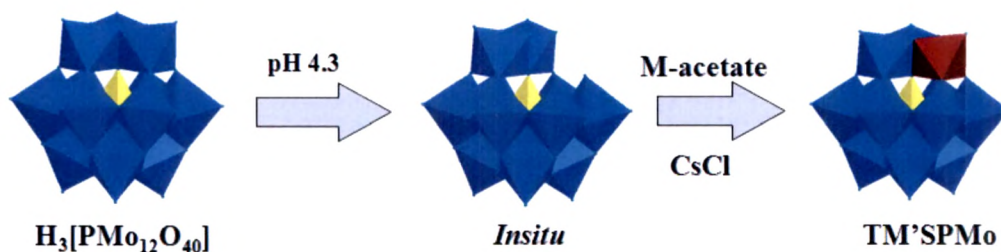
A literature survey shows that, all reported articles describe syntheses of the  $\text{Co}(\text{II})/\text{Mn}(\text{II})$ -substituted phosphomolybdates either in two steps or from the individual transition metal salts (Scheme 1).



**Scheme 1.** (a) synthesis and isolation of lacunary precursor,  $\text{PMo}_{11}\text{O}_{39}^{7-}$  from either parent  $\text{H}_3\text{PMo}_{12}\text{O}_{40}$  or individual transition metal salts (b) synthesis  $\text{TM}'\text{SPMo}$  by incorporation of transition metal ions into  $\text{PMo}_{11}\text{O}_{39}^{7-}$

In addition, only two reports i.e. either layer or chain structures are available. At the same time, only one report describes synthesis of Ni(II)-substituted phosphomolybdates. No report describing discrete Keggin structures for the cesium salt of Co(II)/Mn(II)/Ni(II)-substituted phosphomolybdate are available in art.

Considering the above aspects, It was thought of interest to develop an easy one-step method (Scheme 2) for the synthesis of Co(II)/Mn(II)/Ni(II)-substituted phosphomolybdate as well as detailed characterization including single-crystal XRD.



**Scheme 2.** One-pot synthesis of TM'SPMo

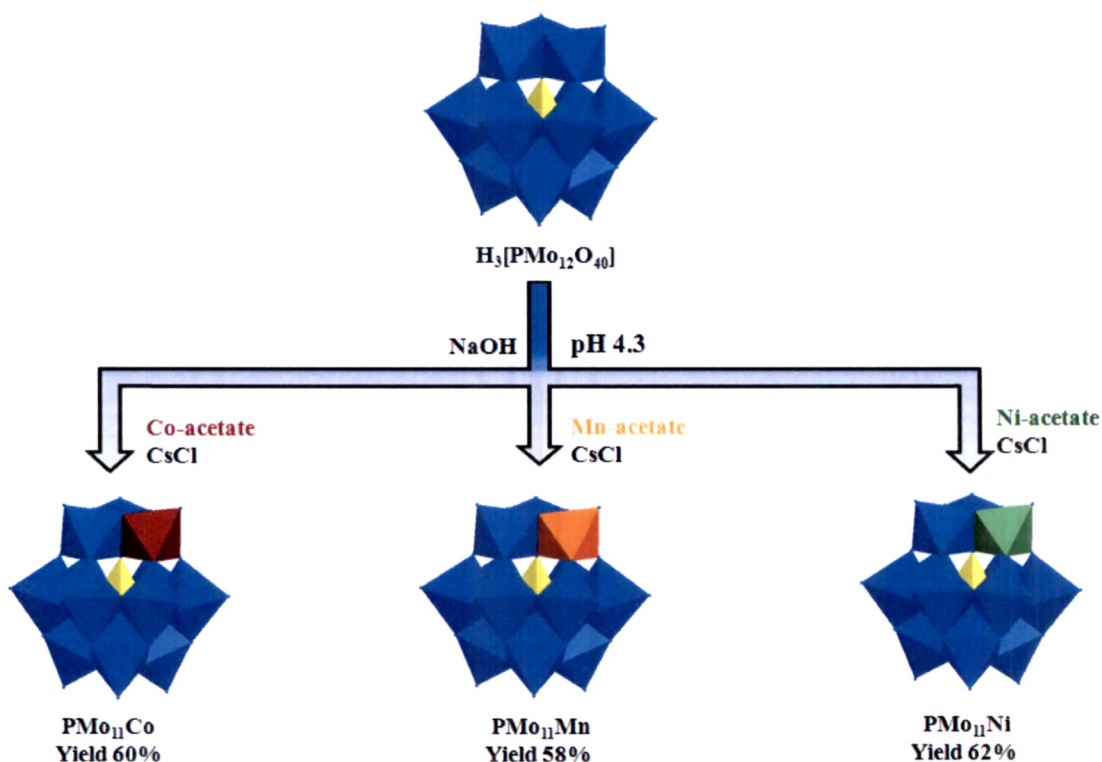
In the present work, for the first time have come up with the one-pot synthesis of the cesium salt of mono transition metal-substituted phosphomolybdate from commercially available 12-molybdophosphoric acid and acetates of the transition metals (Co, Mn, Ni). The synthesized complexes were characterized by elemental analysis (EDX), Single-crystal X-ray diffraction, Thermal analysis (TG-DTA), powder X-ray diffraction (XRD), Fourier Transform Infrared Spectroscopy (FT-IR), Diffused Reflectance Spectra (DRS), electron spin resonance (ESR), and  $^{31}\text{P}$  Magic-Angle Spinning Nuclear Magnetic Resonance ( $^{31}\text{P}$  MAS- NMR).

## EXPERIMENTAL

### Materials

All chemicals used were of A. R. grade. All chemicals used were of A. R. grade. 12-Molybdophosphoric acid ( $\text{H}_3\text{PMo}_{12}\text{O}_{40}$ ;  $\text{PMo}_{12}$ ) sodium hydroxide,  $\text{Na}_2\text{MoO}_4 \cdot 2\text{H}_2\text{O}$   $\text{Co}(\text{CH}_3\text{COO})_2 \cdot 4\text{H}_2\text{O}$ ,  $\text{Mn}(\text{CH}_3\text{COO})_2 \cdot 4\text{H}_2\text{O}$ ,  $\text{Ni}(\text{CH}_3\text{COO})_2 \cdot 4\text{H}_2\text{O}$ ,  $\text{CsCl}$  were obtained from Merck and used as received.

### Synthesis of transition metal substituted phosphomolybdates ( $\text{PMo}_{11}\text{M}$ ; $\text{M}=\text{Co}, \text{Mn}, \text{Ni}$ ) (Scheme 3)



Scheme 3. Synthesis of  $\text{PMo}_{11}\text{M}$  ( $\text{M}=\text{Co}, \text{Mn}, \text{Ni}$ )

### **Synthesis of Co(II) substituted phosphomolybdate (PMo<sub>11</sub>Co):**

Co(II)- substituted phosphomolybdate was synthesized using following procedure. The pH of a solution of H<sub>3</sub>PMo<sub>12</sub>O<sub>40</sub> (1.825 g, 1 mmole) in water (5 mL) was adjusted to 4.3 using NaOH. The solution was heated to 80° C with stirring. A solution of Cobalt acetate (0.249 g, 1 mmole) in water (5 mL) was added to this hot solution. The final pH of the solution was 4.3. The solution was heated at 80° C with stirring for 1 h and filtered hot. A saturated solution of CsCl was added to the hot filtrate. The resulting mixture was allowed to stand overnight at room temperature. The obtained dark reddish brown X-ray quality crystals (yield 60%) were filtered, air dried and designated as PMo<sub>11</sub>Co. The filtrate was used for the estimation of Molybdenum and Cobalt.

### **Synthesis of Mn(II) substituted phosphomolybdate (PMo<sub>11</sub>Mn):**

Same procedure was followed for synthesis of Mn(II)- substituted phosphomolybdate. Instead of Cobalt acetate, 0.245 gm Mn-acetate was added. The obtained dark brown X-ray quality crystals (yield 58%) were filtered, air dried and designated as PMo<sub>11</sub>Mn. The filtrate was used for the estimation of Molybdenum and Manganese.

### **Synthesis of Ni(II) substituted phosphomolybdate (PMo<sub>11</sub>Ni):**

Same procedure was followed for synthesis of Ni(II)- substituted phosphomolybdate. Instead of Cobalt acetate, 0.247 gm Ni-acetate was added. The obtained tiny crystals (yield 62%) were designated as PMo<sub>11</sub>Ni. The filtrate was used for the estimation of Molybdenum and Nickel.

However, after several attempts, we are not succeeded in obtaining good quality crystals, suitable for single crystal X-ray analysis.

## RESULTS AND DISCUSSION

### Characterization of $\text{PMo}_{11}\text{Co}$ and $\text{PMo}_{11}\text{Mn}$

#### Elemental Analysis

$\text{PMo}_{11}\text{Co}$  and  $\text{PMo}_{11}\text{Mn}$  were isolated as the cesium salt after completion of the reaction and the remaining solution was filtered off. The filtrate was analyzed for molybdenum gravimetrically; cobalt and manganese volumetrically [24]. The observed proportion of Mo in the filtrate was 0.5 %, which corresponds to loss of one equivalent of Mo from  $\text{H}_3\text{PMo}_{12}\text{O}_{40}$ . The proportion Co and Mn in the filtrate was 0.0235 % and 0.0231 %, corresponding to incorporation of one equivalent of Co and Mn into the lacunary species created by the removal of one Mo, respectively.

The observed EDX values for the elemental analysis of the isolated complexes were in good agreement with the theoretical values.

For  $\text{PMo}_{11}\text{Co}$ : Anal Calc % : Cs, 25.88; Mo, 41.20; P, 1.20; Co, 2.30; O, 28.75. Found % : Cs, 25.90; Mo, 41.29; P, 1.16; Co, 2.33; O, 28.69.

For  $\text{PMo}_{11}\text{Mn}$ : Anal Calc %: Cs, 26.00; Mo, 41.29; P, 1.21; Mn, 2.15; O, 28.79. Found %: Cs, 26.34; Mo, 41.40 ; P, 1.18; Mn, 2.04; O, 28.61.

#### Crystal structure and Thermal analysis

The single crystal X-ray data was collected on a BRUKER SMART APEX CCD area detector system. [ $\lambda$  (Mo- $\text{K}\alpha$  = 0.71073 Å)] graphite monochromator, two thousand frames were recorded with an  $\omega$  scan width of 0.3°, each for 10s, crystal detector distance 60mm, collimator 0.5mm. The data were reduced by using SAINTPLUS [25] and a multi scan absorption correction using SADABS [25] was performed. Structure solution and refinement were done using programs of



SHELX-97 [26]. All non hydrogen were refined anisotropically. The details of the crystal data are presented in Table 1.

**Table 1** Crystal data and collection parameters for  $\text{PMo}_{11}\text{Co}$  and  $\text{PMo}_{11}\text{Mn}$

	<b><math>\text{PMo}_{11}\text{Co}</math></b>	<b><math>\text{PMo}_{11}\text{Mn}</math></b>
Empirical formula	$\text{Cs}_5 \text{Mo}_{11} \text{Co O}_{46} \text{P}$	$\text{Cs}_5 \text{Mo}_{11} \text{Mn O}_{46} \text{P}$
Formula weight	2559.74	2555.74
Crystal system, space group	Tertagonal , P42/ncm	Tertagonal , P42/ncm
Unit cell dimensions	a= b= 20.7451(12) c= 10.3976(13) $\alpha = \beta = \gamma = 90 \text{ deg}$	a= b = 20.7353(8) A c=10.3479(8) A $\alpha = \beta = \gamma = 90 \text{ deg}$
Temperature	298(2)	110(2) K
Volume	4474.7(7)	4449.1(4) A <sup>3</sup>
Z	4	4
Density (calculated)	4.031 Mg/m <sup>3</sup>	4.054 Mg/m <sup>3</sup>
Absorption coefficient	8.205 mm <sup>-1</sup>	8.252 mm <sup>-1</sup>
F(000)	4868	4868
Crystal size	0.45 x 0.20 x 0.08 mm	0.24 x 0.12 x 0.04 mm
Theta range for data collection	2.40 to 27.73 deg.	1.96 to 27.49 deg.
Reflections collected/unique	20941/ 2057 [R(int) = 0.0280]	21013/ 2652 [R(int) = 0.0294]
Refinement method	Full-matrix least-squares on F <sup>2</sup>	Full-matrix least-squares on F <sup>2</sup>
Goodness-of-fit on F2	1.322	1.214
Final R indices [I <sub>2</sub> σ(I)]	R1 = 0.0967, wR2 = 0.1942	R1 = 0.0688, wR2 = 0.1892
R indices (all data)	R1 = 0.0948, wR2 = 0.1931	R1 = 0.0695, wR2 = 0.1897

The crystal structure analysis of both complexes shows that cobalt and manganese atoms are not present as counter cations. The Cs atoms were present as counter cations with Cs-P distance of 8.338 and 10.517 Å. The crystallographic refinement of the  $\text{PMo}_{11}\text{Co}$  and  $\text{PMo}_{11}\text{Mn}$  suggests the presence of 5.44 and 6 Cs atoms per Keggin unit as counter ions, while the elemental

analysis confirms the presence of 5 Cs atoms for each polyanion respectively. Due to the large difference in the electron densities of H and Mo, the presence of H could not be confirmed from the structural data.

The % of H<sub>2</sub>O was calculated from the TGA curve (Figure 1) (using the same formula given in the Chapter 2, Page 49); the total observed weight loss (4.83 %) at 150° C corresponds to loss of 7H<sub>2</sub>O molecules, for both the complexes.

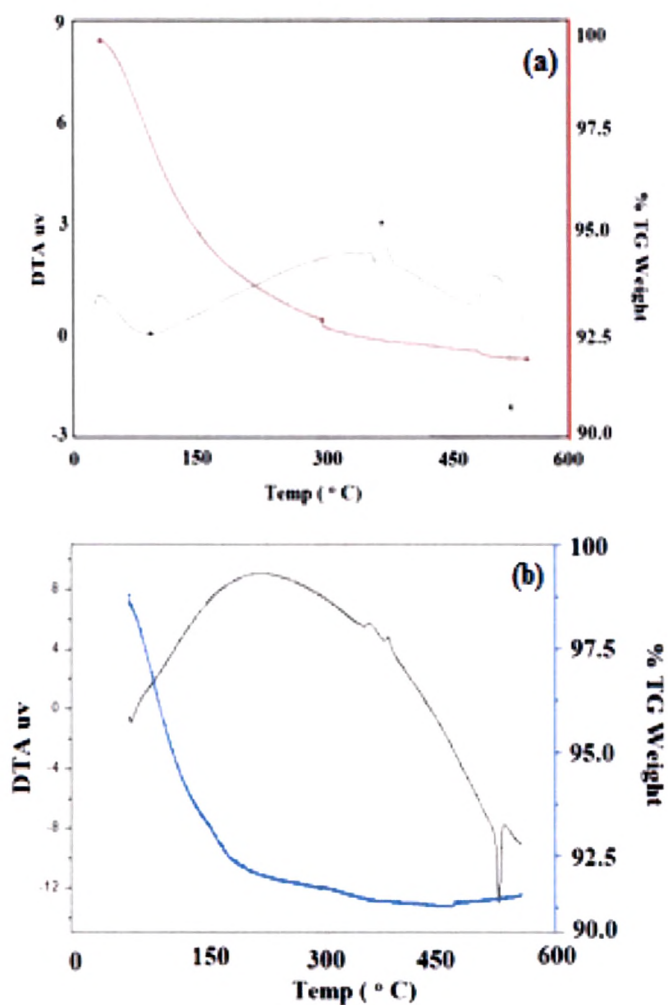
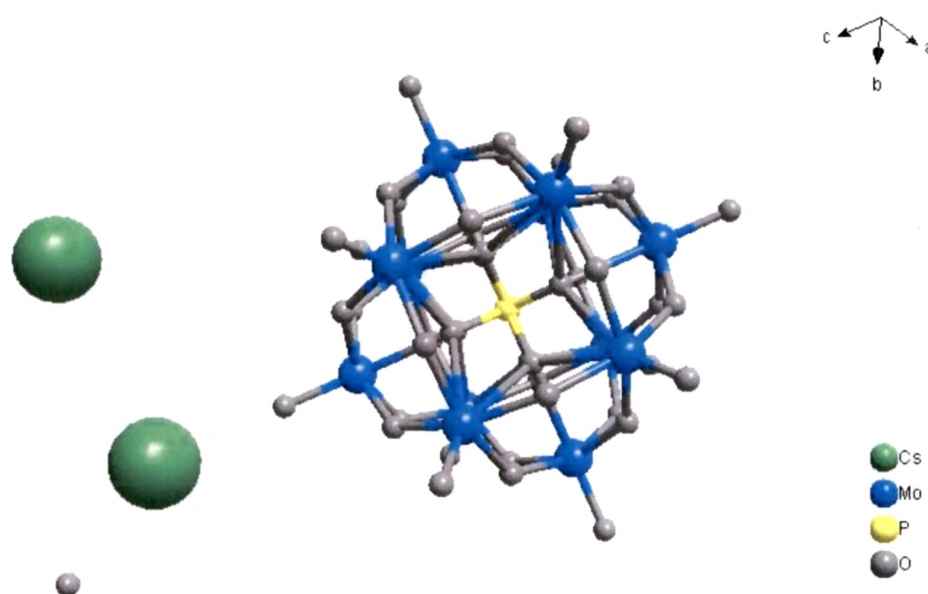


Figure 1. TG-DTA curve (a) PMo<sub>11</sub>Co and (b) PMo<sub>11</sub>Mn

DTA of both complexes showed an endothermic peak in the region 60-150 °C due to water of crystallization. Exothermic peaks in the region 360 °C and 415-430 °C were observed, which may be due to decomposition of Keggin unit and formation of corresponding metal oxides respectively.

Thus, based on the structural, elemental analysis and thermal analysis, the formula of the complexes are proposed as  $\text{Cs}_5[\text{PCo}(\text{H}_2\text{O})\text{Mo}_{11}\text{O}_{39}]\cdot 6\text{H}_2\text{O}$  and  $\text{Cs}_5[\text{PMn}(\text{H}_2\text{O})\text{Mo}_{11}\text{O}_{39}]\cdot 6\text{H}_2\text{O}$ .

The structural analysis of complexes shows two types of disorders in the crystal (Figure 2).



**Figure 2.** Disordered Keggin type structure

(i) In  $\text{PMo}_{11}\text{Co}$ , Co was distributed over the 12 positions and the Co atom could not be distinguished from the 11 Mo atoms distributed equally over the 12 addenda atoms in the Keggin structure, and (ii) the Keggin polyanion is distributed over two orientations related by a centre of symmetry [27-29]. Similar disorder is observed for  $\text{PMo}_{11}\text{Mn}$ .

The packing structure of the both the complexes indicates that the Cs atoms occupy the voids created due to the close packing (Figure 3).

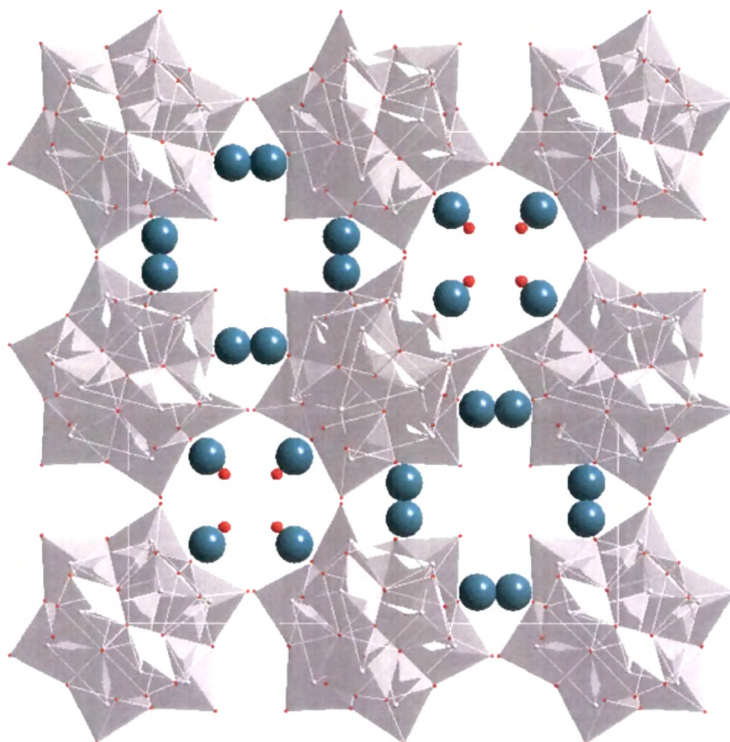


**Figure 3.** Packing diagram

At the same time, H<sub>2</sub>O molecules are also expected to be present in the voids and are interconnected via weak H-bonds. During the final refinement cycle, the isotropic thermal parameters for the atomic coordinates of O indicated the presence of different O atoms, apart from the O atoms of the Keggin unit. These O atoms are thought to originate from the adsorbed water molecules.

The typical Keggin structure in three different types of Mo-O bond distances correspond to the O-terminal (1.70 Å), O-cis bridging (1.90 Å) and O-trans bridging (2.46 Å) atoms, respectively. In the Keggin-type POMs, the central tetrahedral PO<sub>4</sub> is surrounded by twelve MoO<sub>6</sub> octahedra in four groups of

Mo<sub>3</sub>O<sub>13</sub> units. If the structure is totally symmetrical, PO<sub>4</sub> has Td symmetry with all P-O bond lengths equal (1.51-1.55 Å).

In the present structure (PMo<sub>11</sub>Co), the central four oxygen atoms (bonded to three Mo atoms and one P atom) are disordered over eight positions, from which three different types of P-O bonds are obtained. Three of these have almost the same bond length of 1.502 and 1.533 Å, respectively, while the fourth P-O bond has a longer length of 1.615 Å (involving O12), indicating a distortion in PO<sub>4</sub> Td symmetry. This may be due to the change in the environment around the corresponding Mo<sub>3</sub>O<sub>13</sub> unit. Hence, the change in the environment due to the substitution of Co in the corresponding Mo<sub>3</sub>O<sub>13</sub> and P-O12-Mo<sub>3</sub>O<sub>13</sub> moieties is as expected. The three Mo atoms attached to O12 are Mo2, Mo2 and Mo4. The bond length of Mo4-O12 is 2.48 Å. The corresponding terminal oxygen attached to Mo4 is O14. So, as mentioned earlier in the discussion, the presence of disorder in the crystal structure is at O14, and hence, the probability of Co substitution is maximum at Mo4. Similarly, in PMo<sub>11</sub>Mn, three different types of P-O bonds are obtained for four P-O bonds. Three of these have almost the same bond length of 1.527 and 1.557 Å, respectively, while the fourth P-O bond has a longer length of 1.619 Å (involving O13), indicating a distortion in PO<sub>4</sub> Td symmetry. The change in the environment due to the substitution of Mn in the corresponding Mo<sub>3</sub>O<sub>13</sub> and P-O13-Mo<sub>3</sub>O<sub>13</sub> moieties is as expected. The three Mo atoms attached to O13 are Mo1, Mo1 and Mo4. The bond length of Mo4-O13 is 2.493 Å. The corresponding terminal oxygen attached to Mo4 is O10. So, as mentioned earlier in the discussion, the presence of disorder in the crystal structure is at O10, and hence, the probability of Mn substitution is maximum at Mo4.

Cs cations show a number of contacts with the anions. It seems likely that extensive cooperation between cations throughout the crystal is important to form a continuous network that stabilizes the structure and makes the crystals stable in air.

The powder XRD pattern of  $\text{PMo}_{11}\text{Co}$  and  $\text{PMo}_{11}\text{Mn}$  along with the simulated pattern using the data set obtained by single crystal analysis is presented in Figure 4.

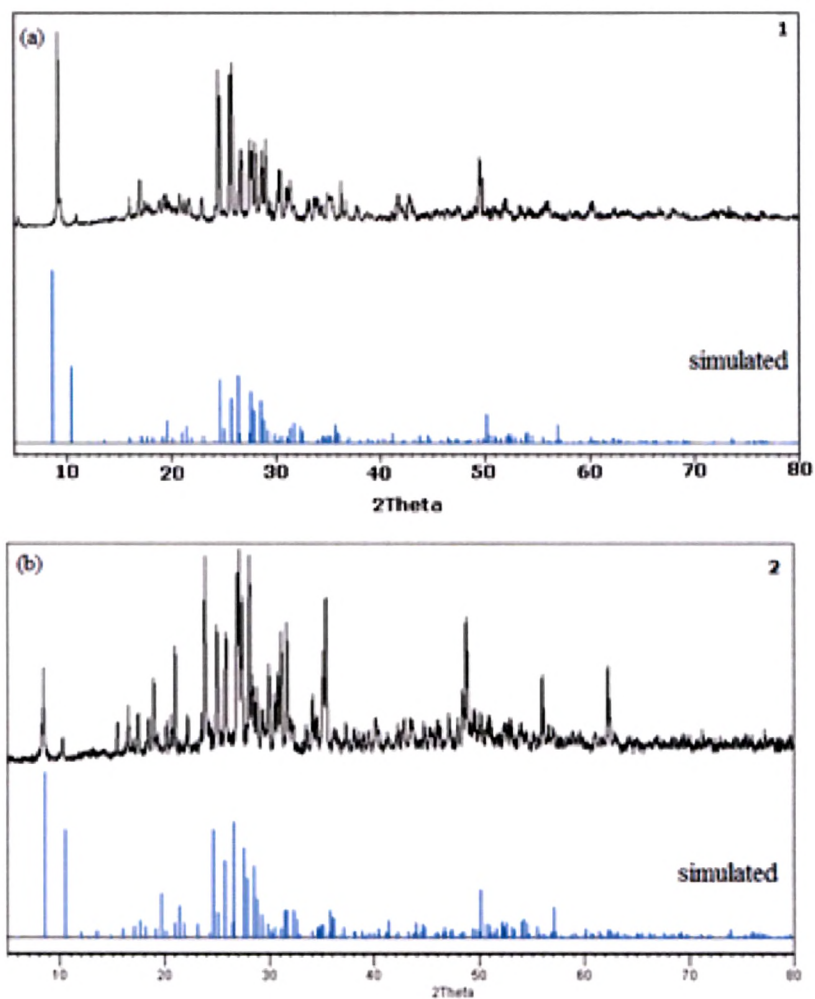


**Figure 4.** Powder XRD and simulated pattern of (a)  $\text{PMo}_{11}\text{Co}$  and (b)  $\text{PMo}_{11}\text{Mn}$

The experimental and simulated patterns are similar indicating that the single crystal and bulk structures are identical.

## Powder XRD

The XRD pattern of  $\text{PMo}_{11}\text{Co}$  and  $\text{PMo}_{11}\text{Mn}$  was totally different from  $\text{PMo}_{12}$  while it resembled  $\text{PMo}_{11}$  confirming the presence of 11Mo atoms in the synthesized complexes (Figure 5).

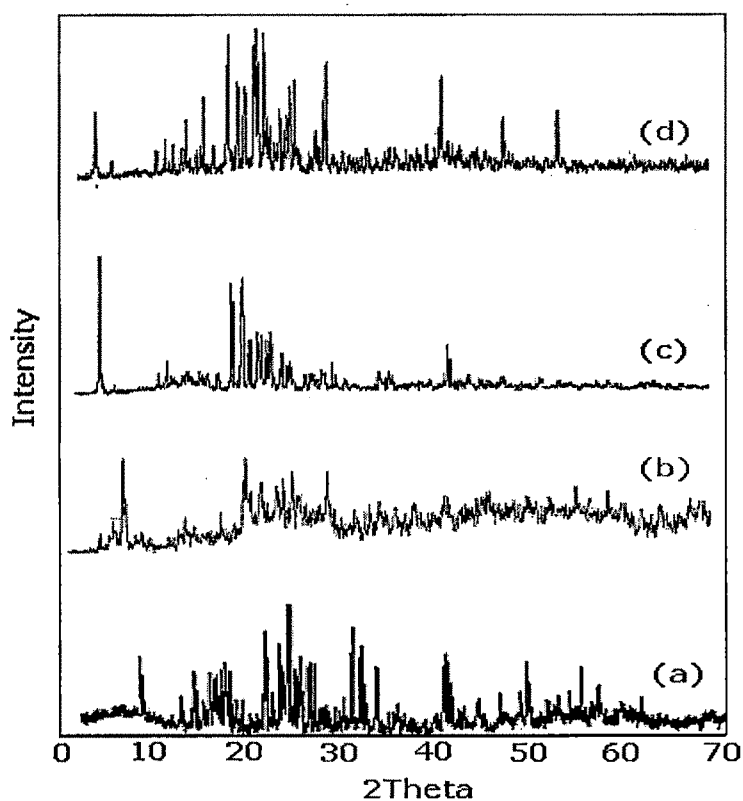


**Figure 5.** Powder X-Ray pattern of (a)  $\text{PMo}_{12}$  (b)  $\text{PMo}_{11}$  (c)  $\text{PMo}_{11}\text{Co}$  and (d)  $\text{PMo}_{11}\text{Mn}$

Along with the characteristic peak of  $\text{PMo}_{11}$ , few additional peaks were found in case of both complexes which may be due to incorporation of transition metal into the lacunary position of phosphomolybdate.

## FT-IR

The FT-IR spectra for  $\text{PMo}_{12}$ ,  $\text{PMo}_{11}$ ,  $\text{PMo}_{11}\text{Co}$  and  $\text{PMo}_{11}\text{Mn}$  are shown in Figure 6. The FT-IR of  $\text{PMo}_{12}$  show bands at  $1070\text{ cm}^{-1}$ ,  $965\text{ cm}^{-1}$  and  $870$  and  $790\text{ cm}^{-1}$  corresponding to the symmetric stretching of P-O, Mo-O and Mo-O-Mo bonds, respectively. The FT-IR spectra show P-O bond frequency  $1050$  and  $1043\text{ cm}^{-1}$  for  $\text{PMo}_{11}\text{Co}$  and  $\text{PMo}_{11}\text{Mn}$  respectively.

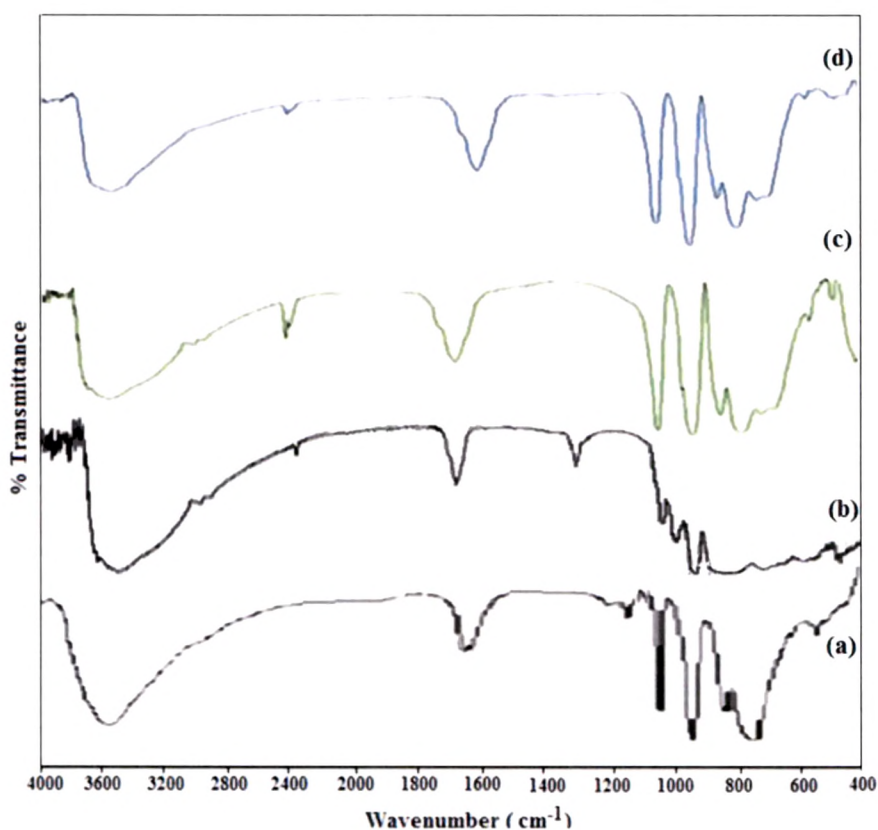


**Figure 6.** FT-IR Spectra of (a)  $\text{PMo}_{12}$  (b)  $\text{PMo}_{11}$  (c)  $\text{PMo}_{11}\text{Co}$  (d)  $\text{PMo}_{11}\text{Mn}$

The FT-IR spectra of  $\text{PMo}_{11}$  shows bands at  $1048$  and  $999\text{ cm}^{-1}$ ,  $935$  and  $906\text{ cm}^{-1}$  and  $855\text{ cm}^{-1}$  attributed to asymmetric stretches of P-O, Mo-Ot and Mo-O-Mo, respectively. The shift in band position as compare to  $\text{PMo}_{12}$  as well as  $\text{PMo}_{11}$  indicates the introduction of transition metal into the octahedral lacuna. A shift in the stretching vibration of Mo=O and Mo-O-Mo for both complexes was also

observed indicating the complexation of the transition metals. An additional band at 480 and 422  $\text{cm}^{-1}$  is attributed to the Co-O, and Mn-O vibration, respectively. Thus, the FT-IR spectra clearly show the incorporation of Co/Mn into the Keggin framework.

## DRS

Figure 7 shows the DRS for  $\text{PMo}_{11}$ ,  $\text{PMo}_{11}\text{Co}$  and  $\text{PMo}_{11}\text{Mn}$ . In case of  $\text{PMo}_{11}$ , intense absorption band at  $\sim 285$  nm are caused due to  $\text{O} \rightarrow \text{Mo}$  charge transfer.

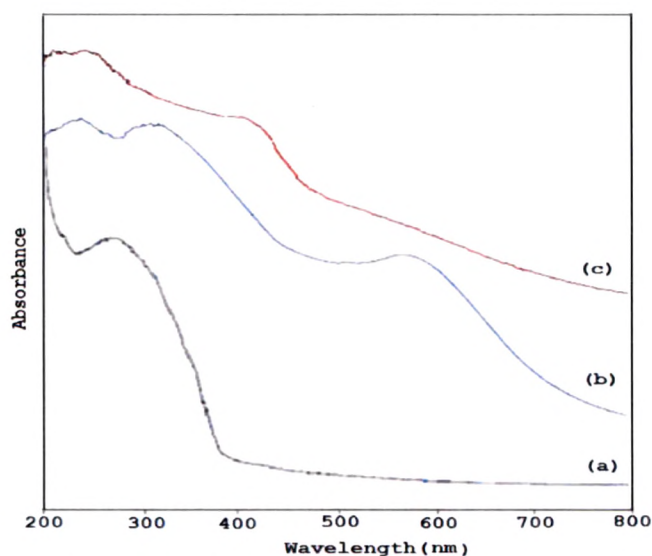


**Figure 7.** DRS of (a)  $\text{PMo}_{11}$  (b)  $\text{PMo}_{11}\text{Co}$  and (c)  $\text{PMo}_{11}\text{Mn}$

The DRS of  $\text{PMo}_{11}\text{Co}$  and  $\text{PMo}_{11}\text{Mn}$  show two peaks. A peak at around 270 nm corresponds to  $\text{O} \rightarrow \text{Mo}$  charge transfer, indicating the formation of  $\text{PMo}_{11}\text{O}_{39}$  lacuna in the synthesized complexes. The observed shifting as compared to that of  $\text{PMo}_{11}$  may be due to the substitution of transition metal. The DRS of  $\text{PMo}_{11}\text{Co}$  and  $\text{PMo}_{11}\text{Mn}$  shows, broad band in the region 560-580 nm and 390-430 nm corresponds to the presence of Co(II) and Mn(II) in the complexes, respectively.

## ESR

Further, the presence of Co(II), and Mn(II) in the synthesized complexes was confirmed by ESR. The full range (3200 - 2000 G) X-band Room temperature ESR spectra (Figure 8) for  $\text{PMo}_{11}\text{Co}$  and  $\text{PMo}_{11}\text{Mn}$  was recorded. ESR spectra of  $\text{PMo}_{11}\text{Co}$  shows eight hyperfine signals ( $\text{Co}^{2+}$ ;  $I=7/2$ ), confirming the presence of paramagnetic Co(II). The observed  $g$  value of  $\sim 2.66$  shows that Co(II) is in octahedral or distorted octahedral environment.

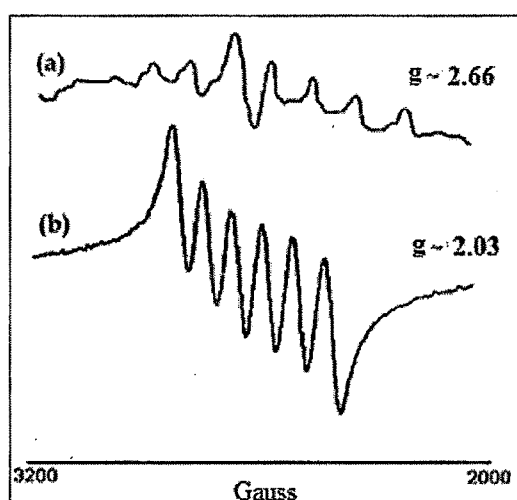


**Figure 8.** ESR spectra of (a)  $\text{PMo}_{11}\text{Co}$  and (b)  $\text{PMo}_{11}\text{Mn}$ .

Similarly, ESR spectra of  $\text{PMo}_{11}\text{Mn}$  shows six signals ( $\text{Mn}^{2+}$ ;  $s=5/2$ ), indicates the presence of Mn(II) with octahedral or distorted octahedral symmetry. It is reported that the  $g$  value of  $\sim 2$  attributed to octahedral or distorted octahedral environment of Mn(II) [8]. The obtained  $g$  value (2.03) is in good agreement with a reported one and confirms the presence of paramagnetic Mn(II).

## $^{31}\text{P}$ MAS NMR

The effect of paramagnetic Co(II) and Mn(II) was also reflected in  $^{31}\text{P}$  MAS NMR. The absence of chemical shift in  $^{31}\text{P}$  MAS NMR of  $\text{PMo}_{11}\text{Co}$  and  $\text{PMo}_{11}\text{Mn}$  is attributed to the paramagnetic effect caused by the presence of paramagnetic Co(II) and Mn(II), respectively [20].

## Characterization of $\text{PMo}_{11}\text{Ni}$

As mentioned earlier, obtained crystals for  $\text{PMo}_{11}\text{Ni}$  are very tiny in size, hence not suitable for Single crystal X-ray analysis.

For first row transition metal substituted phosphomolybdates,  $\text{PMo}_{11}\text{Co}$  and  $\text{PMo}_{11}\text{Mn}$ , Single crystal X-ray analysis showed structural disorders in Keggin unit. As nickel is from the same series, we are expecting the identical disordered structure for  $\text{PMo}_{11}\text{Ni}$ . However,  $\text{PMo}_{11}\text{Ni}$  was characterized with elemental, thermal as well as spectral analysis.

## Elemental Analysis

$\text{PMo}_{11}\text{Ni}$  was isolated as the cesium salt after completion of the reaction and the remaining solution was filtered off. The filtrate was analyzed for molybdenum gravimetrically; Nickel volumetrically [24]. The observed proportion of Mo in the filtrate was 0.5 %, which corresponds to loss of one equivalent of Mo from  $\text{H}_3\text{PMo}_{12}\text{O}_{40}$ . The proportion Ni in the filtrate was 0.0233 % corresponding to incorporation of one equivalent of nickel into the lacunary species created by the removal of one Mo, respectively. The observed EDX value for the elemental analysis of the isolated complex was in good agreement with the theoretical values.

Anal Calc % : Cs, 26.03; Mo, 41.34; P, 1.21; Ni, 2.30; O, 28.84. Found % : Cs, 26.12; Mo, 41.39; P, 1.24; Ni, 2.32; O, 28.89.

## TG-DTA

TGA of  $\text{PMo}_{11}\text{Ni}$  shows initial weight loss of 4.33% upto 50-150 °C. This may be due to the removal of adsorbed water and water of crystallization. Number of water molecules was calculated from TGA using the same formula given in

Chapter 2, Page 49. Similarly, DTA shows an endothermic peak at around 130-140 °C, due to loss of water of crystallization. An exothermic peak in the region 425 °C indicates decomposition of Keggin unit.

Thus, based on elemental and thermal analysis, the formula of the complex is proposed as  $\text{Cs}_5[\text{PNi}(\text{H}_2\text{O})\text{Mo}_{11}\text{O}_{39}]\cdot 6\text{H}_2\text{O}$ .

### Powder XRD

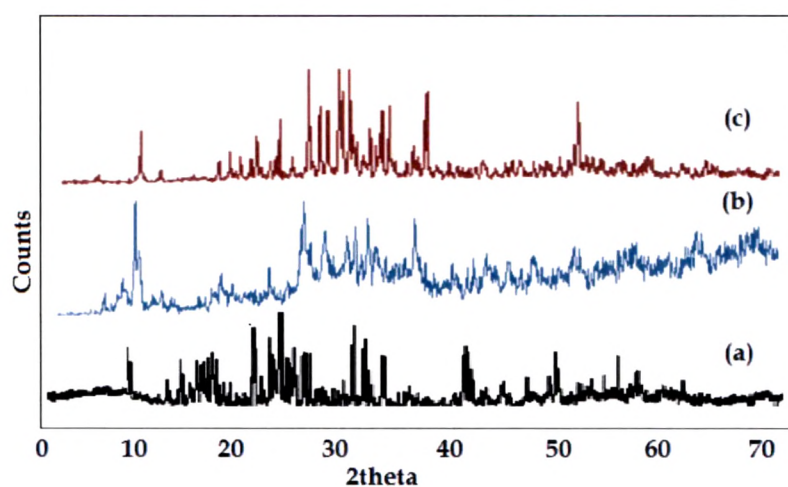


**Figure 9.** XRD pattern of (a)  $\text{PMo}_{12}$ , (b)  $\text{PMo}_{11}$  and (c)  $\text{PMo}_{11}\text{Ni}$

The powder X-ray diffraction pattern of  $\text{PMo}_{12}$ ,  $\text{PMo}_{11}$ , and  $\text{PMo}_{11}\text{Ni}$  are shown in Figure 9. It is seen from Figure 9. That  $\text{PMo}_{12}$  shows characteristic peaks between 10 to 30  $2\theta$ , indicating presence of parent Keggin ion. It is also seen from Figure 9 that, XRD pattern of  $\text{PMo}_{11}\text{Ni}$  are entirely different as compare to  $\text{PMo}_{12}$ , but similar to  $\text{PMo}_{11}$ . This confirms that the synthesized material contains  $\text{PMo}_{11}$ . Slight shifting in  $2\theta$  peak value as compare to that of  $\text{PMo}_{11}$  may be due to the substitution of Ni. Moreover, XRD pattern of  $\text{PMo}_{11}\text{Ni}$  shows that the synthesized material is crystalline in nature.

## FT-IR

The frequencies of FT-IR bands for  $\text{PMo}_{12}$ ,  $\text{PMo}_{11}$  and  $\text{PMo}_{11}\text{Ni}$  are shown in Figure 10. The FT-IR of  $\text{PMo}_{12}$  showed bands at  $1070\text{ cm}^{-1}$ ,  $965\text{ cm}^{-1}$  and  $870$  and  $790\text{ cm}^{-1}$  corresponding to the symmetric stretching of P-O, Mo-O and Mo-O-Mo bonds respectively. The FT-IR spectra of  $\text{PMo}_{11}$  shows bands at  $1048$  and  $999\text{ cm}^{-1}$ ,  $935$  and  $906\text{ cm}^{-1}$  and  $855\text{ cm}^{-1}$  attributed to asymmetric stretches of P-O, Mo-Ot and Mo-O-Mo, respectively.

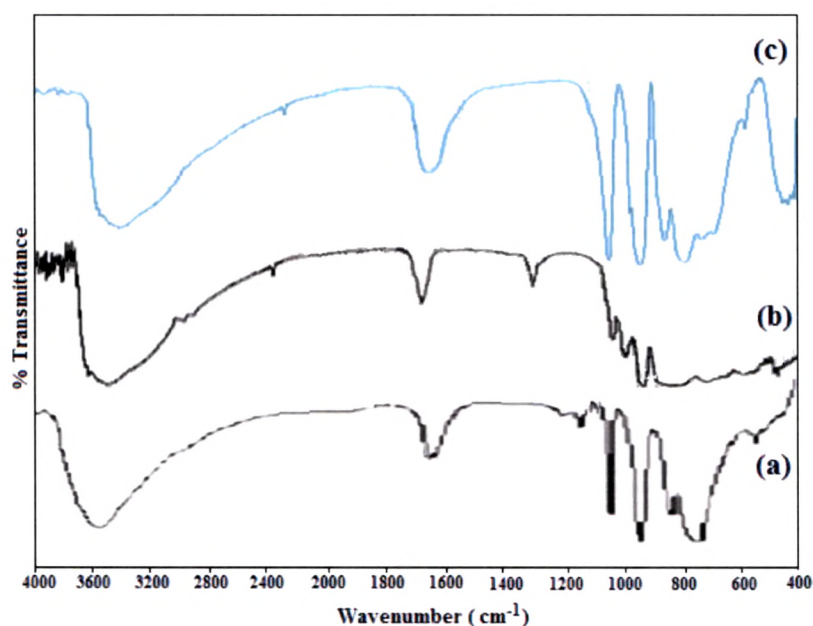


**Figure 10.** FT-IR of (a)  $\text{PMo}_{12}$ , (b)  $\text{PMo}_{11}$  and (c)  $\text{PMo}_{11}\text{Ni}$

The FT-IR spectra of  $\text{PMo}_{11}\text{Ni}$  showed P-O bond frequency  $1046\text{ cm}^{-1}$ . The shift in band position as compare to  $\text{PMo}_{12}$  as well as  $\text{PMo}_{11}$  indicates that transition metal was introduced into the octahedral lacuna. There is also a shift in the stretching vibration of Mo=O and Mo-O-Mo, indicating the complexation of the transition metals. An additional band  $442\text{ cm}^{-1}$  is attributed to Ni-O vibration. Thus, the FT-IR spectra clearly show the incorporation of Ni into the Keggin framework.

## DRS

The DRS gives information about the non-reduced heteropolyanions due to charge transfer from oxygen to metal. DR spectra of  $\text{PMo}_{11}$  exhibit absorption at 290 nm ( $\lambda_{\text{max}}$ ) is attributed to O $\rightarrow$ Mo charge transfer (Figure 11). Similar O $\rightarrow$ Mo charge transfer band at 300 nm was observed for  $\text{PMo}_{11}\text{Ni}$ . In addition, a broad peak at 550-600 nm was obtained in  $\text{PMo}_{11}\text{Ni}$  which arises due to the d-d transitions typical for octahedral transition metals with six oxygen bond ligands.

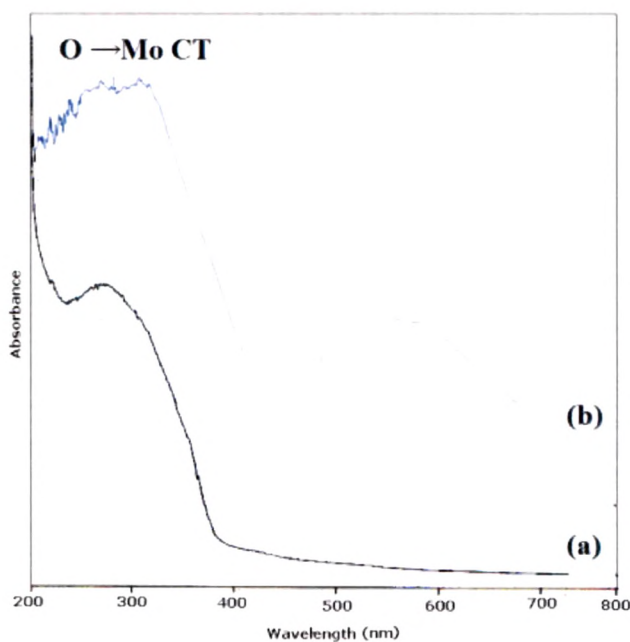


**Figure 11.** DRS of (a)  $\text{PMo}_{11}$  and (b)  $\text{PMo}_{11}\text{Ni}$

## $^{31}\text{P}$ MAS NMR

The effect of paramagnetic Ni(II) was also reflected in  $^{31}\text{P}$  MAS NMR. The absence of chemical shift of  $^{31}\text{P}$  MAS NMR of  $\text{PMo}_{11}\text{Ni}$  is attributed to the paramagnetic effect caused by the presence of paramagnetic Ni(II).

## CONCLUSIONS

1. We, for the first time, have introduced one-step synthesis and crystal structure of Keggin-type Cs-salts of  $\text{PMo}_{11}\text{M}$  ( $\text{M}=\text{Co}, \text{Mn}, \text{Ni}$ ) starting from the commercially available  $\text{PMo}_{12}$ .
2. The single crystal analysis shows double disorder in the crystal: (i) the transition metal (Co/Mn) and Mo atoms were distributed over the 12 positions and the transition metal (Co/Mn) could not be distinguished from the 11Mo atoms distributed equally over the 12 addenda atoms in the Keggin structure (ii) the Keggin polyanion is distributed over the two orientations related by a centre of symmetry. For  $\text{PMo}_{11}\text{Ni}$ , we were not succeeded to obtain good quality crystal suitable for Single crystal X-ray analysis.
3. The presence of transition metal (Co/Mn/Ni) was confirmed by FT-IR, DRS, ESR as well as  $^{31}\text{P}$  NMR.
4. The present synthesis method provides a new easy and simple route to develop novel materials based on other transition metals-substituted phosphomolybdates.

## REFERENCES

1. J. M. Thomas, R. Raja. *Top. Catal.*, 40, 3 (2006).
2. O. A. Kholdeeva. *Top. Catal.*, 40, 229 (2006).
3. C. L. Hill, R. B. Brown. *J. Am. Chem. Soc.*, 108, 536 (1986).
4. T. J. R. Weakley, S. A. Malik. *J. Inorg. Nucl. Chem.*, 29, 2935 (1967).
5. C. M. Torne, G. F. Tourne, S. A. Malik, T. J. R. Weakly. *J. Inorg. Nucl. Chem.*, 32, 3875 (1970).
6. J. R. Galan-Mascaros, C. Gimenez-Saiz, S. Triki, C. J. Gomez-Garcia, E. Coronado, L. Ouahab. *Angew. Chem. Int. Ed. Engl.*, 34, 1460 (1995).
7. X. Zhang, M. T. Pope, M. R. Chance, G. B. Jameson. *Polyhedron*, 14, 1381 (1995).
8. C. L. Hill, C. M. Prosser-McCartha. *Coord. Chem. Rev.*, 143, 407 (1995).
9. M. Sadakane, E. Steckhan. *J. Mol. Catal A: Chem.*, 114, 221 (1996).
10. J. R. Galan-Mascaros, C. Gimenez-Saiz, S. Triki, C. J. Gomez-Garcia, E. Coronado. *J. Am. Chem. Soc.*, 120, 4671 (1998).
11. K. Nowinska, A. Waclaw, W. Masierak, A. Gutsze. *Catal. Lett.*, 92, 157 (2004).
12. M. S. S. Balula, I. Santos, J. A. F. Gamelas, A. M. V. Cavaleiro, N. Binsted, W. Schlindwein. *Eur. J. Inorg. Chem.*, 1027 (2007).
13. D. E. Katsoulis, M. T. Pope. *J. Am. Chem. Soc.*, 106, 2737 (1984).
14. D. E. Katsoulis, M. T. Pope. *J. Chem. Soc., Chem. Commun.*, 1186 (1986).
15. D. E. Katsoulis, M. T. Pope. *J. Chem. Soc., Dalton Trans.*, 1483 (1989).
16. L. A. Combs-Walker, C. L. Hill. *Inorg. Chem.*, 30, 4016 (1991).
17. R. Nuemann, M. Dahan, *J. Chem. Soc. Chem. Commun.*, 2277, (1995).
18. R. Karcz, K. Pamin, J. Poltowicz, J. Haber, *Catal. Lett.* 132, 159, (2009).
19. X. Lin, G. Gao, L. Xu, F. Li, L. Liu, N. Jiang, Y. Yang. *Solid State Sci.*, 11, 1433 (2009).

20. T. Mazari, C.R. Marchal, S. Hocine, N. Salhi, C. Rabia. *J. Nat. Gas Chem.*, 18, 319 (2009).
21. E. Coronado, J.R. Galan-Mascaros, C. Gimenez-Saiz, C.J. Gomez-Garcia, S. Triki. *J. Am. Chem. Soc.*, 120, 4671 (1998).
22. J. Hu, R.C. Burns. *J. Mol. Catal. A: Chem.*, 184, 451 (2002).
23. T. A. G. Duarte, I.C. M. S. Santos, M. M. Q. Simões, M. G. P. M. S. Neves, A. M. V. Cavaleiro, J. A. S. Cavaleiro, *Catal. Lett.*, (2013) in press
24. A. Vogel. *A Textbook of Quantitative Inorganic Analysis*, 2nd Edn, Longmans, Green and Co., London (1951).
25. Bruker. SADABS, SMART, SAINT and SHELXTL, Bruker AXS Inc., Madison, WI, USA (2000).
26. G.M. Sheldrick. SHELX-97, Program for Crystal Structure Solution and Analysis, University of Gottingen, Gottingen, Germany (1997).
27. T.J.R. Weakly. *J. Crystall. Spec. Res.*, 17, 383 (1987).
28. R. F. Klevtsova, E. N. Yarchenko, L. A. Glinskaya, L. I. Kuznetsova, L. G. Detusheva, T. P. Lazarenko. *Zh. Strukt. Khim.*, 32, 102 (1991).
29. M. Sadakane, D. Tuskuma, M.H. Dickman, U. Kortz, M. Higashijima, W. Ueda. *Dalton Trans.*, 4271 (2006).